

This document was prepared in conjunction with work accomplished under Contract No. DE-AC09-96SR18500 with the U. S. Department of Energy.

DISCLAIMER

This report was prepared as an account of work sponsored by an agency of the United States Government. Neither the United States Government nor any agency thereof, nor any of their employees, nor any of their contractors, subcontractors or their employees, makes any warranty, express or implied, or assumes any legal liability or responsibility for the accuracy, completeness, or any third party's use or the results of such use of any information, apparatus, product, or process disclosed, or represents that its use would not infringe privately owned rights. Reference herein to any specific commercial product, process, or service by trade name, trademark, manufacturer, or otherwise, does not necessarily constitute or imply its endorsement, recommendation, or favoring by the United States Government or any agency thereof or its contractors or subcontractors. The views and opinions of authors expressed herein do not necessarily state or reflect those of the United States Government or any agency thereof.

Key Words:
condensate
falling droplet
heat transfer
immiscible liquid

Retention:
Permanent

HEAT TRANSFER FROM CONDENSATE DROPLETS FALLING THROUGH AN
IMMISCIBLE LAYER OF TRIBUTYL PHOSPHATE

J. E. Laurinat

AUGUST, 2005

Westinghouse Savannah River Company
Savannah River Site
Aiken, SC 29808

**Prepared for the U.S. Department of Energy Under
Contract Number DE-AC09-96SR18500**



DISCLAIMER

This report was prepared for the United States Department of Energy under Contract No. DE-AC09-96SR18500 and is an account of work performed under that contract. Neither the United States Department of Energy, nor WSRC, nor any of their employees makes any warranty, expressed or implied, or assumes any legal liability or responsibility for accuracy, completeness, or usefulness, of any information, apparatus, or product or process disclosed herein or represents that its use will not infringe privately owned rights. Reference herein to any specific commercial product, process, or service by trade name, trademark, name, manufacturer or otherwise does not necessarily constitute or imply endorsement, recommendation, or favoring of same by Westinghouse Savannah River Company or by the United States Government or any agency thereof. The views and opinions of the authors expressed herein do not necessarily state or reflect those of the United States Government or any agency thereof.

Printed in the United States of America

**Prepared For
U.S. Department of Energy**

Heat Transfer from Condensate Droplets Falling Through an Immiscible Layer of Tributyl Phosphate

James E. Laurinat, Savannah River National Laboratory, Aiken, SC 29808

Abstract

As part of a safety analysis of reactions in two-layer mixtures of nitric acid and tributyl phosphate (TBP), an experiment was conducted to study how steam condensate mixes with the TBP layer when steam passes over a TBP-nitric acid mixture. The experiments showed that the condensate does not form a separate layer on top of the TBP but instead percolates as droplets through the TBP layer. The temperature at the top surface of the TBP layer undergoes a step change increase when the initial condensate droplets reach the surface. Temperatures at the surface and within the TBP and aqueous layers subsequently approach a steady state distribution governed by laminar convection and radiation heat transfer from the vapor space above the two-layer mixture. The rate of temperature increase and the steady state temperature gradient are determined by a characteristic propagation velocity and a streamwise dispersion coefficient for heat transfer. The propagation velocity is the geometric mean of the thermal convection velocities for the organic and aqueous phases, and the dispersion coefficient equals 0.494 times the product of the superficial condensate droplet velocity and the diameter of the test vessel. The value of the dispersion coefficient agrees with the Joshi (1980) correlation for liquid phase backmixing in bubble columns. Transient perturbations occur in the TBP layer temperatures. A Fourier analysis shows that the dominant frequency of these perturbations equals the natural frequency given by the transient heat transfer solution.

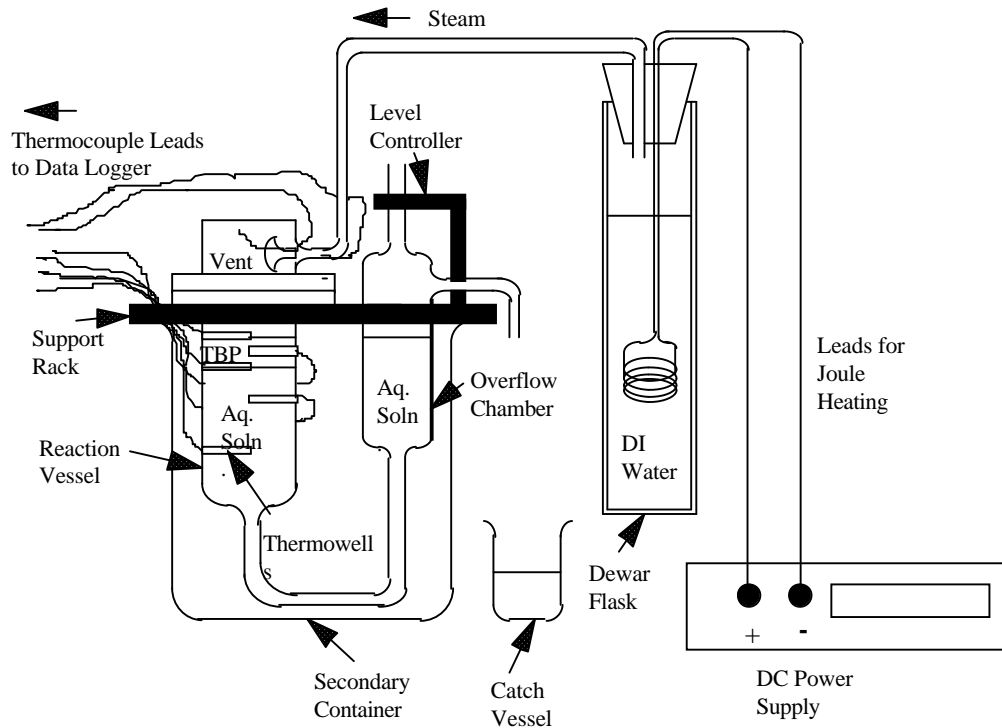
1.0 Introduction and Summary

A study of heat transfer due to condensate dripping through an immiscible organic liquid follows. This study was prompted by safety concerns about a potential runaway reaction between nitric acid and tributyl phosphate (TBP), which forms an immiscible organic layer above aqueous nitric acid solutions. TBP is used as a complexant to separate actinide elements dissolved in nitric acid. The reaction between nitric acid and TBP is highly exothermic and generates potentially explosive product gases. At elevated temperatures, this reaction undergoes a thermal excursion if there is not enough residual aqueous solution dissolved in the TBP to moderate the heat of reaction by its evaporation. Thus, the temperature, the pressure, and the degree of mixing of aqueous components in the TBP layer determine whether or not a given two-layer nitric acid-TBP mixture can be safely stored.

Various mechanisms for heating the TBP layer have been considered. One of these mechanisms is steam condensate dripping onto and percolating through the TBP layer. With steam condensate heating, the nitric acid-TBP reaction, if it occurs, would proceed most rapidly at the top of the TBP layer. The bubbling reaction zone would not necessarily extend down to the TBP-nitric acid interface, so the acid layer might not replenish the water lost by evaporation. To address this concern, an experiment was conducted to study how steam condensate mixes with the TBP layer when steam passes over a TBP-nitric acid mixture.

2.0 Description of Experiments

Figure 1 depicts the apparatus for the steam heating experiment. As this figure shows, a voltage source heated water to generate steam in a Dewar flask. The source generated 30 watts of power. A mixture of steam and condensate from the Dewar traveled through an insulated tube to a glass mixing vessel containing a two-layer TBP-nitric acid mixture. A flexible tube connected the bottom of this glass vessel to an overflow chamber, which maintained a constant liquid level as condensate entered the vessel. The mixing vessel contained thermowells to measure the temperature of the TBP and nitric acid layers.



Note: The Steam line from the Dewar flask to the reaction vessel was insulated with glass wool, and the secondary vessel also contained glass wool insulation. This insulation is not shown.

Figure 1. View of Experimental Apparatus, Including Mixing Vessel, Overflow Chamber, Dewar Flask, and Power Source.

Both the mixing vessel and the overflow chamber were set inside a wide mouth beaker that served as a secondary containment vessel and a container for insulation material. Except for a small viewing area, the sides and bottom of the mixing vessel and the overflow chamber were wrapped with glass wool in an effort to minimize heat losses. The top of the mixing vessel was uncovered so that it could be cooled by natural convection to the surrounding air. In Figure 1, the glass wool insulation is not shown to permit a clear view of the mixing vessel and the overflow chamber.

The mixing vessel had an ID of 0.0572 m and a height of 0.222 m. Glass thermowells were located 0.1080 , 0.0984, 0.0889, 0.0794, and 0.0445 m from the bottom of the vessel.

During the test the vessel was filled to a level even with the top thermowell, which corresponds to a volume of about $2.75 \times 10^{-4} \text{ m}^3$. Of this total, the TBP layer occupied the top 0.0191 m, corresponding to a volume of approximately $5.0 \times 10^{-5} \text{ m}^3$. This placed the middle thermowell approximately at the TBP-nitric acid interface. The overflow chamber contained an additional $8.0 \times 10^{-5} \text{ m}^3$ of nitric acid when filled to the overflow spout.

The thermowells contained Type T thermocouples, which are suitable for temperatures ranging from 273 to 473 K. Additional thermocouples were added to measure the temperature in the steam inlet tube and the temperature in the middle of the vapor space at the top of the glass vessel. The thermocouples were connected to a computer via a panel of Keithley Metrobyte[®] transducers. The computer logged temperatures at 100-second intervals, using Labtech Notebook[©] computer software.

The voltage output from the thermocouples was adjusted to give temperatures in °C using nominal calibration multipliers supplied by Keithley Metrobyte[®]. The thermocouples were calibrated using a 373 K boiling solution of deionized water, but the calibration results were not applied during data collection. Instead, these results were applied during subsequent data analyses.

To start the experiments, a nitric acid-saturated TBP layer was prepared by mixing 50 ml of reagent grade TBP with $1.50 \times 10^{-4} \text{ m}^3$ of a 50 weight % nitric acid mixture in a stirred vessel for about 1-2 minutes. The TBP and nitric acid layers were allowed to separate and were then added to the mixing vessel. An additional $2.00 \times 10^{-4} \text{ m}^3$ of 50 weight % nitric acid was prepared and added to fill the vessel and the overflow chamber until the TBP layer just covered the top thermowell. The Dewar flask was filled with 296 K distilled water and the electrical power source was turned on to heat this water to generate steam.

After an initial interval during which the water in the Dewar was heated to the boiling temperature, steam generation began. The steam flowed into the mixing vessel largely as condensate at the boiling point of water (373 K). Virtually all of the steam condensed either in the transfer tube before entering the mixing vessel or on the walls of the mixing vessel. The condensate formed droplets which traveled down the side walls before entering the TBP layer. The condensate flowed through the TBP layer as droplets with an apparent diameter of about 0.003 m. No visible layer of condensate formed on top of the TBP. It was verified through a rough heat balance calculation that the electrical power source was almost 100% efficient in generating either steam or condensate. The volume of condensate exiting the overflow chamber was almost equal to the electrical power divided by the density and heat of vaporization of water.

There was no visible vapor formation in either the TBP or nitric acid layer during the experiment. This was taken as evidence that any TBP decomposition reaction that occurred did not proceed at a significant rate.

Figure 2 depicts the temperature transients for the condensate heating experiment. As was observed for the vapor space in the previous experiment, the steam inlet temperature underwent a step function change from ambient temperature (296 K) to the steam saturation temperature as steam generation began. Surface level control was improved in this experiment. Consequently, the temperature at the TBP surface also approached the

saturation temperature relatively rapidly. Temperatures further down in the TBP layer and in the nitric acid layer increased more slowly and in fact seemed to level off before approaching the saturation temperature. This indicates that there were significant heat losses from the mixing vessel. The thermocouple measuring the temperature in the vapor space had an intermittent open circuit failure, so that temperature is not shown. The surface temperature appeared to fluctuate at more or less regular intervals. Table 1 lists the conditions for this experiment.

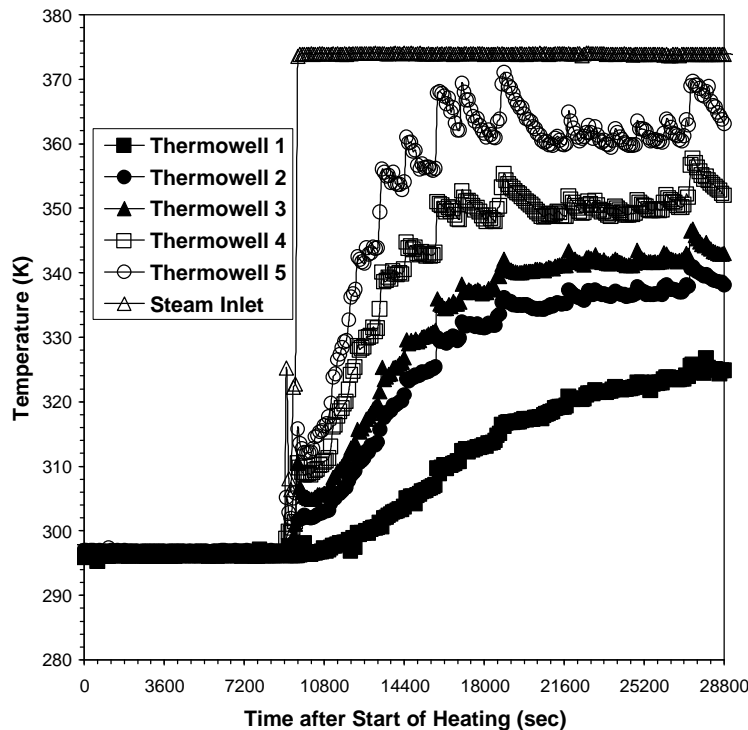


Figure 2. Temperature Transients during Steam Heating Experiment.

Table 1. Experimental Conditions

Diameter	0.0572 m
Height	0.2223 m
Steam or condensate flow rate	1.36×10^{-5} kg/sec
Superficial velocity of condensate in the TBP layer	5.2×10^{-6} m/sec

3.0 Model of Droplet Flow, Reaction, and Heat Transfer in the TBP Layer

The steam heating experiment did not provide a direct measurement of the effect of condensate droplets on the TBP-nitric acid reaction because the temperatures were too low for the reaction to occur to any measurable extent. Instead, the experiment was used to indirectly measure a dispersion coefficient for mixing induced by the droplets. This dispersion coefficient could then be used in a model to calculate temperature and composition transients for

steam heating of a TBP-nitric acid system at higher temperatures. The following sections describe the calculation of the dispersion coefficient for droplet mixing and its use in the heat and mass balances for the TBP-nitric acid reaction. Terms in the equations presented in these sections are defined in the Nomenclature.

3.1 Calculation of the Dispersion Coefficient for Condensate Droplet Mixing

The dispersion coefficient is calculated from a model fit to the measured steady state temperature profile for the second experiment. The model fit is based on the steady state solution to the one-dimensional heat transfer equations for the TBP and aqueous layers. Since the experiment was conducted at a relatively low temperature, where the rate of reaction between TBP and nitric acid is negligible, the reaction term was dropped from these equations.

The heat transfer equation for the TBP layer is written for the TBP phase. This equation takes the form:

$$\frac{\partial T}{\partial t} = \alpha \frac{\partial^2 T}{\partial z^2} \quad (1)$$

where α is a dispersion coefficient. The dispersion coefficient is the sum of the molecular dispersivity, α_m , and an axial dispersivity, $\alpha_{t,d}$, that accounts for the condensate droplet flow:

$$\alpha = \alpha_m + \alpha_{t,d} \quad (2)$$

where

$$\alpha_m = \frac{k_m}{\rho C_p} \quad (3)$$

and

$$\alpha_{t,d} = \frac{k_{t,d}}{\rho C_p} \quad (4)$$

Because the TBP phase is stationary, the heat transfer equation for the TBP layer does not contain a velocity term to account for condensate droplet flow. However, the droplet velocity is modeled through the axial dispersion coefficient, $\alpha_{t,d}$. Axial dispersion for liquid droplets falling through quiescent liquid layers has not been widely studied. For this reason, a correlation for liquid backmixing in bubble columns is adapted to model the axial dispersion. To be useful in modeling droplet mixing, the bubble column mixing correlation must be defined in terms of the velocity of the liquid phase entrained by the bubbles. One such correlation was proposed by Joshi (1980). The Joshi correlation takes the form

$$\alpha_b = c_b d_b v_{l,c} \quad (5)$$

where α_b is the dispersion coefficient for bubble mixing of the liquid layer, d_b is the bubble column diameter, $v_{l,c}$ is the superficial circulation velocity of the liquid entrained by the bubble flow, and c_b is a constant. Joshi obtained values of c_b ranging between 0.29 and 0.33 for correlations of different sets of data.

The liquid circulation velocity for droplet flow includes both the flow rate of the droplets and the added mass of the continuous phase entrained by the droplets. For laminar (Stokes) flow, the added mass occupies half of the droplet volume (Darwin, 1953). It follows that the liquid circulation velocity for falling droplets is 1.5 times the superficial droplet velocity. With these considerations, the correlation for the axial dispersion coefficient for the droplet flow becomes

$$\alpha_{t,d} = 1.5c_d d v_{sd} \quad (6)$$

where v_{sd} is the superficial droplet velocity and c_d is a coefficient which should be numerically equal to c_b .

One may note that the dispersion coefficient is correlated with the vessel diameter even though the depth of the TBP layer is considerably shallower than the diameter. The justification for the use of the diameter as the length scale is the fact that the droplets penetrate the TBP-aqueous interface, so that this interface does not pose an impediment to heat transfer.

The heat added by the droplets appears in the surface boundary condition, which, at steady state, equates the dispersion of heat within the TBP layer to the sum of the sensible heat transfer between the condensate droplets and the TBP phase, the thermal radiation between the walls of the glass vessel and the TBP surface, and conduction through the vapor space above the TBP layer. This condition is given by

$$-\frac{\alpha}{v_{sd}} \frac{dT}{dz} = St(T_{sat} - T) \quad (7)$$

where T_{sat} is the saturation temperature of the condensate droplets. The heat transfer parameters in this expression are grouped in a Stanton number, St , defined as the ratio of heat transfer to the surface to convection away from the surface:

$$St = \frac{\rho_c c_{p,c} v_{sd} + h_{rad} + \frac{k_{m,v}}{H}}{\rho_c c_p v_{sd}} \quad (8)$$

where h_{rad} is a radiation heat transfer coefficient and $\frac{k_{m,v}}{H}$ is a laminar convection heat transfer coefficient for the vapor space above the TBP layer.

The radiation heat transfer coefficient, in turn, is given by

$$h_{rad} = \sigma \epsilon_0 \frac{\epsilon_{glass} (T_{sat}^4 - T_0^4)}{T_{sat} - T_0} \quad (9)$$

The heat transfer equation for the aqueous layer is

$$\frac{\partial T}{\partial t} = \alpha_{aq} \frac{\partial^2 T}{\partial z^2} - v_{sd} \frac{\partial T}{\partial z} \quad (10)$$

where, as was the case for the TBP phase, the dispersion coefficient α_{aq} is expressed as the sum of molecular and axial dispersivities:

$$\alpha_{aq} = \alpha_{m,aq} + \alpha_{t,d,aq} \quad (11)$$

$$\alpha_{m,aq} = \frac{k_{m,aq}}{\rho_{aq} c_{p,aq}} \quad (12)$$

and

$$\alpha_{t,d,aq} = \frac{k_{t,d,aq}}{\rho_{aq} c_{p,aq}} \quad (13)$$

The turbulent dispersion coefficient for the aqueous layer, $\alpha_{t,d,aq}$, is correlated identically as the coefficient for the TBP layer:

$$\alpha_{t,d,aq} = 1.5 c_d d v_{sd} \quad (14)$$

The same coefficient is used for both layers.

Steady state heat transfer solutions for the TBP and aqueous phase are obtained by setting the time dependent terms in Equations 1 and 10 equal to zero and specifying the following temperatures at the TBP surface:

$$T = T_0 \text{ at } z = 0 \quad (15)$$

the TBP-aqueous interface:

$$T = T_i \text{ at } z = h \tag{16}$$

and at the bottom of the aqueous layer:

$$T = T_b \text{ at } z = h_{aq} \tag{17}$$

Application of these conditions yields the following solutions for the temperatures in the TBP layer:

$$T = T_0 - St(T_{sat} - T_0) \frac{v_{sd}z}{\alpha} \tag{18}$$

and in the aqueous layer:

$$T = \frac{T_i \left(\exp\left(\frac{v_{sd}(z-h)}{\alpha_{aq}}\right) - \exp\left(\frac{v_{sd}(h_{aq}-h)}{\alpha_{aq}}\right) \right) + T_b \left(1 - \exp\left(\frac{v_{sd}(z-h)}{\alpha_{aq}}\right) \right)}{1 - \exp\left(\frac{v_{sd}(h_{aq}-h)}{\alpha_{aq}}\right)} \tag{19}$$

Finally, the interfacial temperature is obtained by equating the TBP and aqueous layer heat fluxes at the interface:

$$\alpha_{aq} \frac{\partial T}{\partial z} \Big|_{aq} = \alpha \frac{\partial T}{\partial z} \Big|_{TBP} \tag{20}$$

Substitution of the aqueous and TBP layer temperatures from Equations 18 and 19, respectively, gives the following expression for T_i .

$$T_i = T_b + St(T_{sat} - T_0) \left(\exp\left(\frac{v_{sd}(h_{aq}-h)}{\alpha_{aq}}\right) - 1 \right) \tag{21}$$

A trial and error fit of the average steady state temperature profile was used to compute the dispersion coefficient c_d . A Stanton number of 3.80 was calculated from Equation 8 and used to fit the data. Figure 3 compares the profile fit with the average measured temperature profile. As this figure shows, the profile fit correlates the measurements reasonably well. The profile fit gives a value of 0.329 for c_d (or an overall coefficient of 0.494 based on the superficial droplet velocity), a surface temperature of 360.5 K (compared to an average measured temperature of 360.9K), an interfacial temperature of 338.7 K, and a temperature of 300.7 K at the bottom of the vessel. The value for c_d agrees with the values for c_b obtained by Joshi for bubble column mixing, which, as one may recall, ranged from 0.29 to 0.33.

3.2 Analytic Solution for Surface Temperature Transient in the Absence of Reaction

A transient solution for the TBP surface temperature is obtained by substituting the surface heat flux condition (Equation 7) in the TBP layer heat transfer equation (Equation 1).

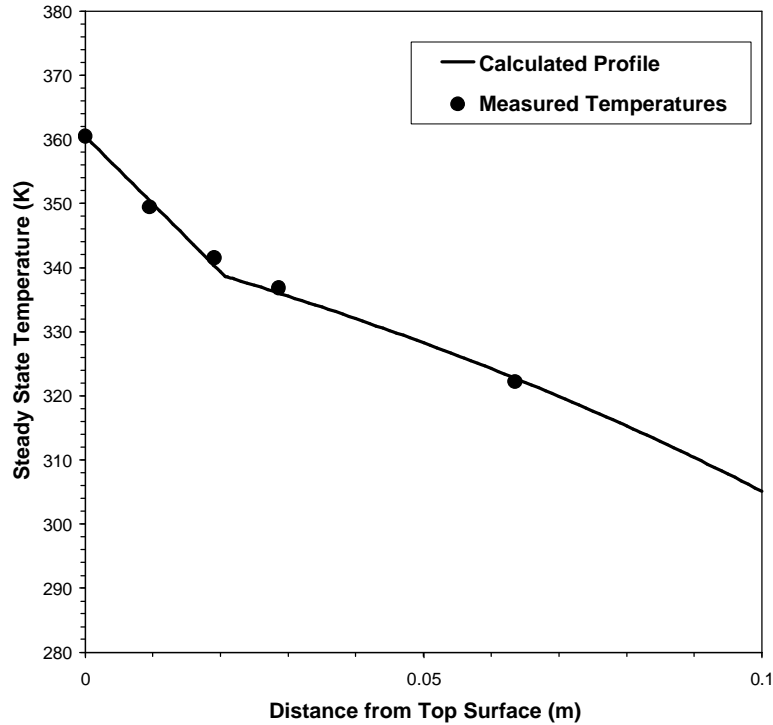


Figure 3. Comparison of Measured and Calculated Steady State Temperatures for Steam Heating Experiment.

This substitution is most easily illustrated using the finite difference form of these equations. The forward time, center step finite difference formulation of the heat transfer equation is

$$\frac{T_j^{n+1} - T_j^n}{\Delta t} = \frac{\alpha}{\Delta z} \left(\frac{T_{j+1}^n - T_j^n}{\Delta z} - \frac{T_j^n - T_{j-1}^n}{\Delta z} \right) \tag{22}$$

where T_j^n is the temperature at the j^{th} node at the n^{th} time step. At the TBP layer surface, $j=1$.

In the solution of the finite difference equations, the heat flux boundary condition is used to compute the temperature gradient for the surface node. This yields

$$\frac{T_1^{n+1} - T_1^n}{\Delta t} = \frac{\alpha}{\Delta z} \left(\frac{T_2^n - T_1^n}{\Delta z} + \frac{v_{sd}}{\alpha} \text{St} (T_s - T_1^n) \right) \tag{23}$$

A straightforward solution of the finite difference equations with this boundary condition gives a much more rapid surface temperature increase than was measured (see Figure 2). This discrepancy arises from an inherent discretization error in the finite difference equations. The

nodal spacing gives an effective convection velocity, $\frac{\alpha}{\Delta z}$, which significantly exceeds the characteristic velocity at which heat is transferred to the TBP layer. This characteristic velocity, v_c , should be the same order of magnitude as the superficial droplet velocity, v_{sd} .

Substitution of v_c for $\frac{\alpha}{\Delta z}$ in the finite difference equation gives

$$\frac{T_1^{n+1} - T_1^n}{\Delta t} = v_c \left(\frac{T_2^n - T_1^n}{\Delta z} + \frac{v_{sd}}{\alpha} \text{St} (T_{\text{sat}} - T_1^n) \right) \quad (24)$$

In the differential limit, this expression becomes

$$\frac{\partial T}{\partial t} = v_c \left(\frac{\partial T}{\partial z} + \frac{v_{sd}}{\alpha} \text{St} (T_{\text{sat}} - T) \right) \quad (25)$$

Equation 25 can be solved simultaneously with the general heat transfer equation (Equation 1) to obtain a transient expression for the surface temperature. The solution of these equations is simplified by subtracting the steady state temperature derived in the previous section, defined as \bar{T} in this analysis, to get a transient temperature component, \hat{T} . Accordingly, let

$$T = \bar{T} + \hat{T} \quad (26)$$

The transient components of Equations 1 and 25 are:

$$\frac{\partial \hat{T}}{\partial t} = \alpha \frac{\partial^2 \hat{T}}{\partial z^2} \quad (27)$$

and

$$\frac{\partial \hat{T}}{\partial t} = v_c \left(\frac{\partial \hat{T}}{\partial z} - \frac{v_{sd}}{\alpha} \text{St} \hat{T} \right) \quad (28)$$

The next step in the solution is to combine these two expressions to solve for the temperature gradient in terms of the temperature. Equations 27 and 28 combine to give

$$\alpha \frac{\partial^2 \hat{T}}{\partial z^2} = v_c \left(\frac{\partial \hat{T}}{\partial z} - \frac{v_{sd}}{\alpha} \text{St} \hat{T} \right) \quad (29)$$

Factoring of this equation yields

$$\frac{\partial \hat{T}}{\partial z} = \left(\frac{v_c}{2\alpha} \pm i \frac{v_c}{2\alpha} \sqrt{4St \frac{v_{sd}}{v_c} - 1} \right) \hat{T} \quad (30)$$

Finally, substitution for $\frac{\partial \hat{T}}{\partial z}$ in Equation 28 produces the ordinary equation

$$\frac{d\hat{T}}{dt} = \left(\frac{v_c^2}{2\alpha} \left(1 - 2St \frac{v_{sd}}{v_c} \right) \pm i \frac{v_c^2}{2\alpha} \sqrt{4St \frac{v_{sd}}{v_c} - 1} \right) \hat{T} \quad (31)$$

The general solution to this equation, in expanded form, is

$$\hat{T} = C_1 (\cos(\theta) + i \sin(\theta)) \exp \left(\frac{v_c^2 t}{2\alpha} \left(1 - 2St \frac{v_{sd}}{v_c} \right) \right) \left(\cos \left(\frac{v_c^2 t}{2\alpha} \sqrt{4St \frac{v_{sd}}{v_c} - 1} \right) \pm i \sin \left(\frac{v_c^2 t}{2\alpha} \sqrt{4St \frac{v_{sd}}{v_c} - 1} \right) \right) \quad (32)$$

This solution has three undetermined parameters, C_1 , θ , and v_c . The parameter θ is a phase angle that accounts for the inability for temperature changes to propagate downstream from the condensate phase into the TBP layer. According to the model assumptions, the condensate droplets are in thermal equilibrium with the TBP phase as they fall through this layer. It follows that thermal fluxes must propagate equally through both the droplet and TBP phases. However, a thermal flux from the condensate phase cannot propagate fully through the TBP phase due to the lower thermal capacity of the TBP. In fact, only a fraction of the heat proportional to the relative thermal capacity, i.e., the product of the density and heat capacity, can enter the TBP phase. This apparent contradiction can be resolved by assigning a phase angle to the temperature solution, where the real component, the cosine, equals the ratio of the thermal capacities of the phases. Thus,

$$\cos(\theta) = \frac{\rho_c c_p}{\rho_c c_{p,c}} \quad (33)$$

and

$$\sin(\theta) = \pm \sqrt{1 - \left(\frac{\rho_c c_p}{\rho_c c_{p,c}} \right)^2} \quad (34)$$

The constant C_1 is evaluated using initial conditions. At $t = 0$, the real part of the transient temperature, \hat{T}_i , is

$$\hat{T}_i = C_1 \cos(\theta) \quad (35)$$

From the definition of \hat{T} ,

$$\hat{T}_i = T_i - T_\infty \tag{36}$$

where T_∞ represents the steady state surface temperature as $t \rightarrow \infty$.

Therefore,

$$C_1 \cos(\theta) = T_i - T_\infty \tag{37}$$

The initial surface temperature should be determined by the relative ability of the TBP phase to transmit sensible heat from the condensate plus thermal radiation and laminar convection from the top surface of the heating vessel. In other words, the initial temperature rise should equal the difference between the saturation temperature and the initial temperature of the solution prior to heating, divided by the Stanton number:

$$T_i = T_0 + \frac{T_{sat} - T_0}{St} \tag{38}$$

The final parameter to be determined is the characteristic propagation velocity. This velocity should be bounded by the thermal convection velocities in the condensate and TBP phases. The thermal convection velocity in the TBP phase is just the superficial droplet velocity. The thermal convection velocity in the condensate is equal to the droplet velocity, multiplied by the ratio of thermal capacities of the two phases. Thus,

$$v_{sd} < v_c < \frac{\rho_c C_{p,c}}{\rho C_p} v_{sd} \tag{39}$$

An intermediate characteristic velocity equal to the geometric mean of the limiting velocities in this inequality:

$$v_c = \sqrt{\frac{\rho_c C_{p,c}}{\rho C_p}} v_{sd} \tag{40}$$

gives the best fit to the measured rate of increase in the temperature. As the solution will show, this choice makes the time constant for the rate of temperature rise a function of the superficial droplet velocity, the thermal conductivity of the TBP phase, and the density and heat capacity of the condensate.

The final solution is obtained by substituting Equations 33, 34, 37, 38, and 40 in Equation 28. This yields

$$T = T_{\infty} - \left(T_{\infty} - T_0 - \frac{T_{\text{sat}} - T_0}{St} \right) \exp\left(\frac{v_{\text{sd}}^2 t}{2b\alpha} (1 - 2St\sqrt{b}) \right) \left(\cos\left(\frac{v_{\text{sd}}^2 t}{2b\alpha} \sqrt{4St\sqrt{b} - 1} \right) + \frac{\sqrt{1-b^2}}{b} \sin\left(\frac{v_{\text{sd}}^2 t}{2b\alpha} \sqrt{4St\sqrt{b} - 1} \right) \right) \quad (41)$$

where

$$b = \frac{\rho C_p}{\rho_c C_{p,c}} \quad (42)$$

As noted previously, the time constant for this solution is

$$\frac{2b\alpha}{v_{\text{sd}}^2} = \frac{2(k_m + k_{t,d})}{\rho_c C_{p,c} v_{\text{sd}}^2} \quad (43)$$

Figure 4 compares the measured surface temperature transient for the second test, starting from the initial stepwise temperature increase, with the predictions of the model developed in this section. As this figure shows, the model accurately predicts temperatures during both the initial portion of the transient and at later times as steady state approaches. These comparisons demonstrate that the steady state solution and the analysis of starting conditions are approximately correct.

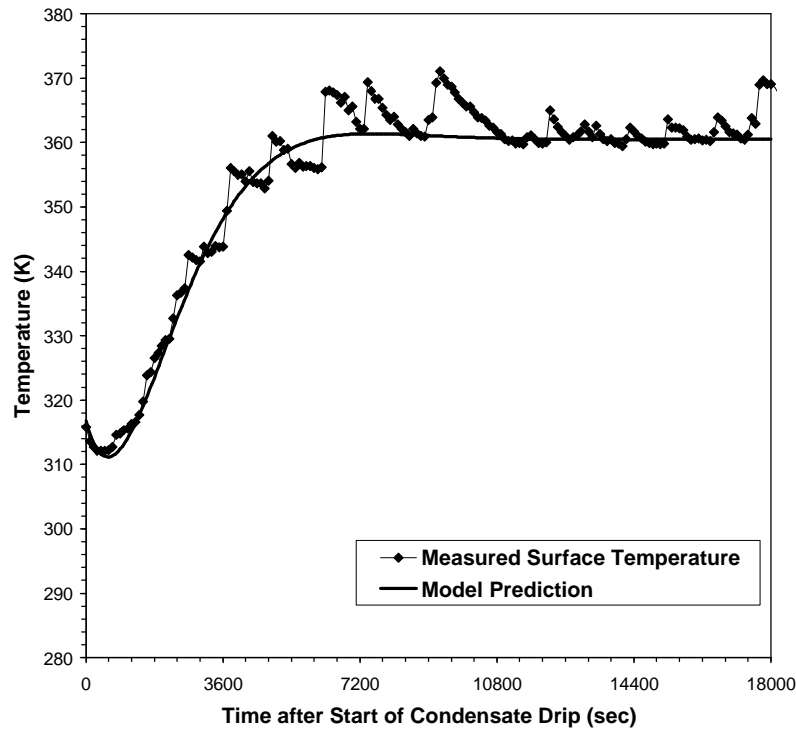


Figure 4. Comparison of Measured and Predicted Temperatures at Top Surface of TBP Layer for Steam Heating Experiment.

During the middle portion of the transient, the measured temperatures fluctuated between the predicted values and the saturation temperature. These fluctuations probably reflect imperfect mixing at the surface. If so, then the frequency of these fluctuations should match the natural frequency governed by the heat transfer conditions at the surface. For the solution of the heat transfer equation (Equation 31), the harmonic frequency is defined by the requirement that the characteristic propagation velocity v_c must remain constant.

Additionally, for the equilibrium solution given by Equation 41, the propagation velocity must match the rate of propagation of heat through the aqueous layer. For temperature fluctuations away from equilibrium, though, the propagation velocity may vary. An examination of Equation 31 reveals that the exponential growth rate for temperature fluctuations increases as the propagation velocity increases, so that fluctuations with larger propagation velocities will predominate over fluctuations with smaller propagation velocities. It follows that the characteristic (or natural) frequency for temperature fluctuations occurs at the maximum possible propagation velocity.

The maximum propagation velocity can be determined by differentiating the harmonic component of the temperature solution, which will be defined as β , with respect to the propagation velocity v_c . (This, of course, presumes that the harmonic frequency is a single-valued function of the propagation velocity, i.e., that only one branch of the quadratic solution for the frequency is valid.) The expression for β is:

$$\beta = \frac{v_c^2}{2\alpha} \sqrt{4St \frac{v_{sd}}{v_c} - 1} \tag{44}$$

The following differentiation

$$\frac{\partial \beta}{\partial v_c} = 0 \text{ at } v_{c,max}, \beta_{max} \tag{45}$$

yields

$$v_{c,max} = 3v_{sd}St \tag{46}$$

so that the maximum, or natural, frequency is given by

$$\beta_{max} = \frac{3\sqrt{3}St^2v_{sd}^2}{2\alpha} \tag{47}$$

The minimum fluctuation time period corresponding to this natural frequency is

$$\tau_{\min} = \frac{2\pi}{\beta_{\max}} \tag{48}$$

The frequency of the fluctuations in the measured surface temperatures can be determined by spectral analysis of the fluctuating component of the temperature transient. Figure 5 depicts the fluctuations in the surface temperatures for the second heating experiment. This figure plots the differences between the measured surface temperatures and the model predictions given by Equation 41. (To minimize any long-term trends in these differences, the linear least squares fit was subtracted.) Figure 6 displays the Fourier transform of these values, converted to the time domain. The Fourier transform exhibits three peaks, one that roughly corresponds to the minimum time period for the natural frequency,

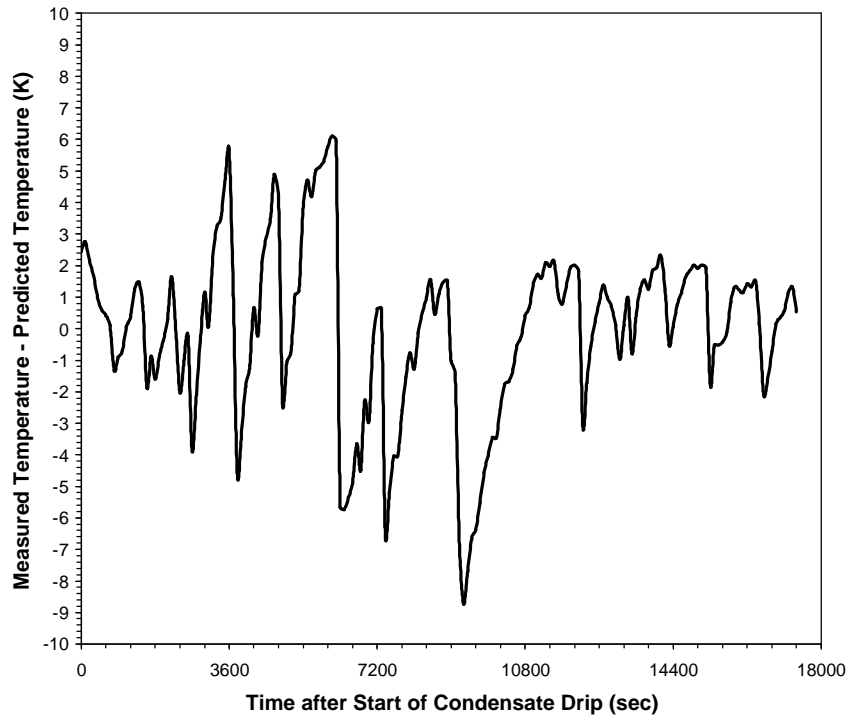


Figure 5. Variation of Difference between Measured and Predicted Temperatures at Top Surface of TBP Layer for Steam Heating Experiment.

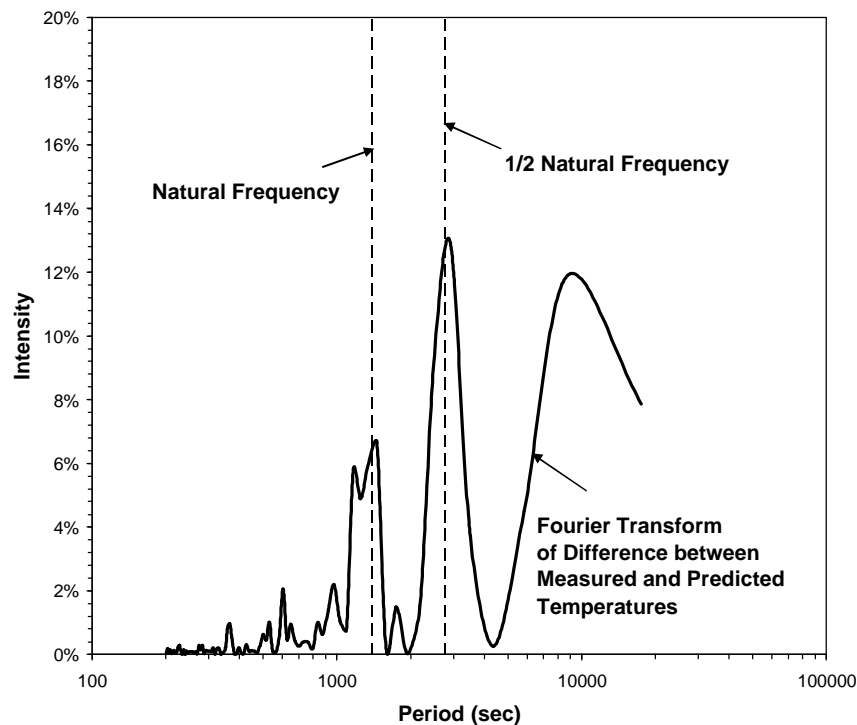


Figure 6. Comparison of Natural Frequency for Temperature Fluctuations for Steam Heating Experiment with Fourier Spectrum for Deviation between Measured and Predicted Surface Temperatures.

expressed by Equation 47, a second at about twice this time period, and a third that is close to the entire time span for the measured data.

A characteristic frequency for the surface temperature fluctuations becomes more apparent in a plot of the second time derivative of the fluctuations, as shown by Figure 7. Taking time derivatives has the effect of a high pass frequency filter, since it amplifies high frequency fluctuations and dampens low frequency trends. This is borne out by the Fourier transforms of the second derivatives. Figure 8 portrays the transforms for the second derivatives of the surface temperature fluctuations, again in the time domain. A comparison of Figures 6 and 8 shows that the peak corresponding to the natural frequency is preserved. However, the Fourier transform for the second time derivative lacks the significant longer time period peaks that appear in the transform shown in Figure 6, but exhibits additional short time period, i.e., high frequency, peaks. These high frequency peaks likely represent sampling noise. To filter out these high frequency signals, a 9-point Savitsky-Galoy filter (Press et al., 1992) was applied to the data in two successive passes. The second pass succeeds in removing the high-frequency noise and isolating the peak corresponding to the natural frequency.

4.0 Conclusions

Experiments were conducted to study how steam condensate mixes with the TBP layer when steam passes over a TBP-nitric acid mixture. The experiments showed that the condensate does not form a separate layer on top of the TBP but instead percolates as

droplets through the TBP layer. The temperature at the top surface of the TBP layer undergoes a step change increase when the initial condensate droplets reach the surface. Temperatures at the surface and within the TBP and aqueous layers subsequently approach a steady state distribution governed by laminar convection and radiation heat transfer from the vapor space above the two-layer mixture. The rate of temperature increase and the steady state temperature gradient are determined by a characteristic propagation velocity and a streamwise dispersion coefficient for heat transfer. The propagation velocity is the geometric mean of the thermal convection velocities for the organic and aqueous phases, and the dispersion coefficient equals 0.494 times the product of the superficial droplet velocity in the TBP layer and the diameter of the test vessel. The value of the dispersion coefficient agrees with the Joshi correlation for liquid phase backmixing in bubble columns. Transient perturbations occur in the TBP layer temperatures. A Fourier analysis shows that the dominant frequency of these perturbations equals the natural frequency given by the transient heat transfer solution.

5.0 Acknowledgements

The assistance of J. R. Smith, who provided suggestions on the experimental setup and furnished the DC power supply and Dewar flask used to generate steam and the computer and software used to log the thermocouple measurements, is greatly appreciated. The work of R. M. Younkings, who designed and built the level controller, and J. G. Dobos and W. C. Sexton, who fabricated the reaction vessel and the overflow chamber, is also appreciated.

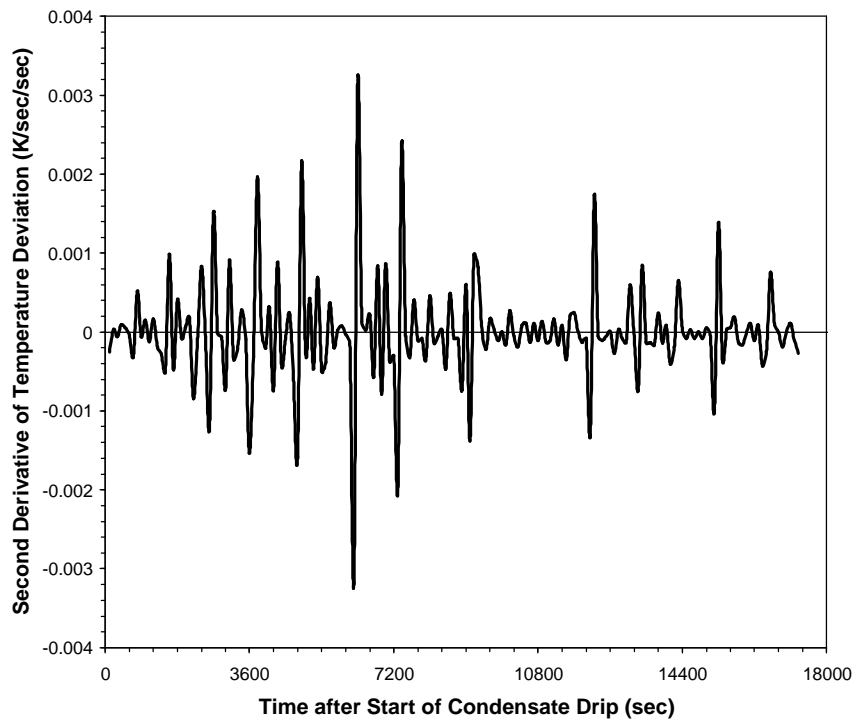


Figure 7. Second Derivative of Variation of Difference between Measured and Predicted Temperatures at Top Surface of TBP Layer for Steam Heating Experiment.

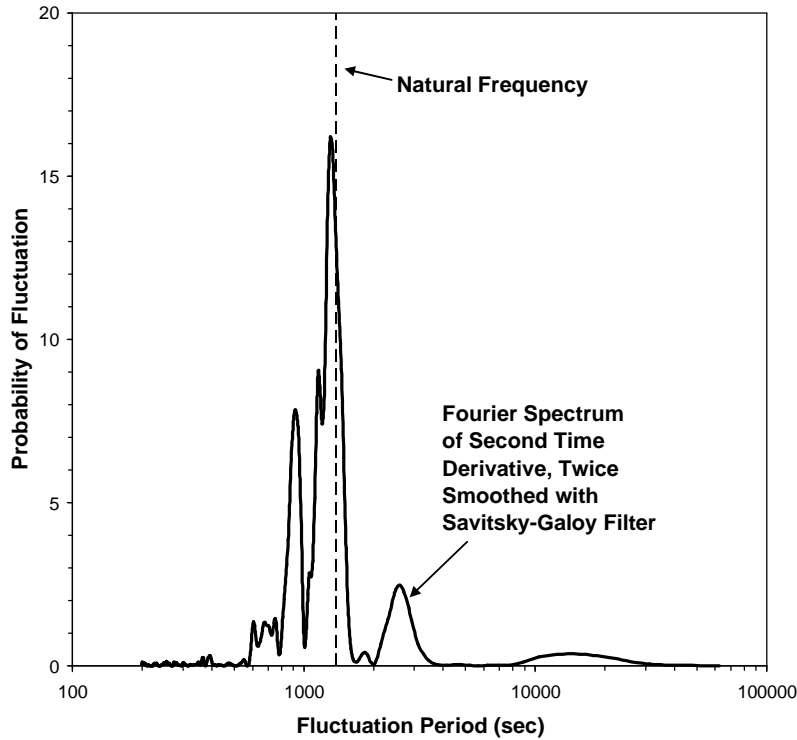


Figure 8. Comparison of Natural Frequency for Temperature Fluctuations for Steam Heating Experiment with Fourier Spectrum for Second Derivative of Difference between Measured and Predicted Temperatures at Top Surface.

6.0 References

J. B. Joshi, "Axial Mixing in Multiphase Contactors – A Unified Correlation," *Trans IChemE*, 58, 155-165, 1980.

C. Darwin, "A Note on Hydrodynamics," *Proc Camb Phil Soc*, 49, 342-352, 1953.

W. H. Press, S. A. Teukolsky, W. T. Vetterling, and B. P. Flannery, Numerical Recipes in Fortran: The Art of Scientific Computing, 2nd ed., Cambridge University Press, Cambridge, England (1992), Chapter 14.8.

7.0 Nomenclature

Variable	Definition
c_b	axial dispersion constant for bubble column backmixing
c_d	axial dispersion constant
c_p	organic phase heat capacity, J/kg/K
$c_{p,aq}$	aqueous phase heat capacity, J/kg/K
$c_{p,c}$	heat capacity of the condensate, J/kg/K
C_1	undetermined coefficient in solution for transient temperature component, K
$C_{1,1}$	undetermined constant in solution for steady state temperature

	component in TBP layer, K
$C_{1,2}$	undetermined constant in solution for steady state temperature
	component in TBP layer, K/m
$C_{2,1}$	undetermined constant in solution for steady state temperature
	component in aqueous layer, K
$C_{2,2}$	undetermined constant in solution for steady state temperature
	component in aqueous layer, K
d	diameter of the test vessel, m
d_b	bubble column diameter, m
h	height of the TBP layer, m
h_{rad}	thermal radiation heat transfer coefficient at the TBP surface, J/m ² /sec/K
H	height of the vapor space in the glass vessel above the TBP surface, m
k_m	organic phase thermal conductivity, J/m/sec/K
$k_{m,aq}$	aqueous phase thermal conductivity, J/m/sec/K
$k_{m,v}$	thermal conductivity of the vapor in the space above the TBP surface, J/m/sec/K
$k_{t,d}$	thermal dispersion coefficient for condensate droplet mixing in the organic phase, J/m/sec/K
$k_{t,d,aq}$	thermal dispersion coefficient for condensate droplet mixing in the aqueous phase, J/m/sec/K

Variable	Definition
St	Stanton number relating heat transferred to the TBP surface to heat removed by convection, defined by Equation 9
t	time, sec
T	temperature, K
\bar{T}	steady state component of the temperature, K
\hat{T}	transient component of the temperature, K
T_{amb}	ambient temperature, K
T_i	initial temperature of the fluid, K
T_j^n	temperature at the j^{th} calculation node at the n^{th} time step, K
T_{sat}	condensate droplet temperature as it enters the TBP layer, K
T_0	temperature at the TBP layer surface, temperature measured by the surface thermocouple, K
T_1	temperature measured by the first thermocouple below the surface, K
T_2	temperature measured by the second thermocouple below the surface, K
T_∞	steady state surface temperature as $t \rightarrow \infty$, K
Δt_i	time interval required to form the heat transfer boundary layer, sec
$\hat{\Delta t}_i$	dimensionless time interval required to form the heat transfer boundary layer
v_c	characteristic velocity for propagation of heat into the TBP layer, m/sec
$v_{c,max}$	maximum characteristic velocity for propagation of heat into the TBP layer at the natural frequency for temperature fluctuations, m/sec
$v_{l,c}$	superficial continuous phase liquid circulation velocity, m/sec
v_{sd}	superficial velocity of the condensate droplets falling through the TBP layer, m/sec
z	distance from the top surface of the TBP layer, m
z_1	distance between the TBP layer surface and the first thermocouple below the surface, m
z_2	distance between the TBP layer surface and the second thermocouple below the surface, m
α	organic phase thermal diffusivity, m^2/sec
α_{aq}	aqueous phase thermal diffusivity, m^2/sec
α_b	axial dispersion coefficient for backmixing in bubble column, m^2/sec
α_m	organic phase molecular thermal diffusivity, m^2/sec
$\alpha_{m,aq}$	aqueous phase molecular thermal diffusivity, m^2/sec
$\alpha_{t,d}$	axial dispersion coefficient for heat transfer in the organic phase, m^2/sec
$\alpha_{t,d,aq}$	axial dispersion coefficient for heat transfer in the aqueous phase, m^2/sec

Variable	Definition
β	frequency for surface temperature fluctuations, radians/sec
β_{\max}	maximum, or natural, frequency for surface temperature fluctuations, radians/sec
ϵ_{glass}	thermal emissivity of the glass vessel
ϵ_0	thermal emissivity of the TBP surface
θ	phase angle for transient component of temperature, defined by Equation 45, radians
ρ	organic phase density, kg/m ³
ρ_{aq}	aqueous phase density, kg/m ³
ρ_c	condensate density, kg/m ³
σ	Boltzmann's constant, 5.67×10^{-8} J/m ² /sec/K ⁴
τ_{\min}	minimum time period for surface temperature fluctuations, sec